MicroRNAs bind to Toll-like receptors to induce prometastatic inflammatory response

Muller Fabbri[a,1,2,3], Alessio Paone[a,2], Federica Calore[a,2], Roberta Galli[a], Eugenio Gaudio[a], Ramasamy Santhanam[a], Francesca Lovat[a], Paolo Fadda[a], Charlene Mao[a], Gerard J. Nuovo[b], Nicola Zanesi[a], Melissa Crawford[c], Gulcin H. Ozer[a], Dorothee Wernicke[a], Hansjuerg Alder[a], Michael A. Caligiuri[d], Patrick Nana-Sinkam[c], Danilo Perrotti[a], and Carlo M. Croce[a,3]

[a]Department of Molecular Virology, Immunology and Medical Genetics and Divisions of [c]Pulmonary, Allergy, Critical Care and Sleep Medicine, and [d]Hematology, The Ohio State University Comprehensive Cancer Center, Columbus, OH 43210; and [b]Phylogeny, Inc., Columbus, OH 43210

Contributed by Carlo M. Croce, June 7, 2012 (sent for review April 20, 2012)

MicroRNAs (miRNAs) are small noncoding RNAs, 19–24 nucleotides in length, that regulate gene expression and are expressed aberrantly in most types of cancer. MiRNAs also have been detected in the blood of cancer patients and can serve as circulating biomarkers. It has been shown that secreted miRNAs within exosomes can be transferred from cell to cell and can regulate gene expression in the receiving cells by canonical binding to their target messenger RNAs. Here we show that tumor-secreted miR-21 and miR-29a also can function by another mechanism, by binding as ligands to receptors of the Toll-like receptor (TLR) family, murine *TLR7* and human TLR8, in immune cells, triggering a TLR-mediated prometastatic inflammatory response that ultimately may lead to tumor growth and metastasis. Thus, by acting as paracrine agonists of TLRs, secreted miRNAs are key regulators of the tumor microenvironment. This mechanism of action of miRNAs is implicated in tumor–immune system communication and is important in tumor growth and spread, thus representing a possible target for cancer treatment.

microvesicles | cytokines | IL-6 | TNF-α

MicroRNAs (miRNAs) are small, noncoding RNAs, 19–24 nt in length, with gene-expression regulatory functions (1, 2) and are expressed aberrantly in most types of cancer (3, 4). MiRNAs also have been detected in the blood of cancer patients (5, 6) and can serve as circulating biomarkers (7). It has been shown that secreted miRNAs within exosomes can be transferred from cell to cell and can regulate gene expression in the receiving cells (8) by canonical binding to their target messenger RNAs (8, 9). More recently, it has been demonstrated that, in addition to their role as gene-expression regulators, miRNAs also directly interact with proteins (10).

Members of the Toll-like receptor (TLR) family (namely, murine *TLR7* and human TLR8) can recognize and bind viral single-stranded RNA (ssRNA) sequences on dendritic cells and B lymphocytes, leading to cell activation and cytokine production (11, 12). TLRs are a family of receptors through which the mammalian innate immune system recognizes the presence of invading pathogens (13, 14). Both murine *TLR7* and human TLR8 bind to and are activated by 20-nt-long ssRNAs, which represent physiological ligands for these two receptors (12), located in intracellular endosomes. Circulating mature miRNAs are 19–24 nt in length and could represent tumor-released ligands of *TLR7* and TLR8 involved in intercellular communication in the tumor microenvironment.

Results and Discussion

Identification of Specific miRNAs Released in Cancer Cell-Derived Exosomes. To identify which miRNAs are present in tumor-secreted exosomes, we isolated exosomes from the supernatant of A-549 and SK-MES lung cancer cell lines. First, we assessed the purified supernatant exosome fraction for enrichment in CD9 and CD63, two known exosome markers (*SI Appendix*, Fig. S1*A*) (8, 15). By performing NanoString analysis, we observed that nine miRNAs (miR-16, -21, -27b, -29a, -133a, –193a-3p, -544, -563, and -1283) were present in exosomes derived from both cell lines at an expression level higher than 50 code counts (Fig. 1*A*). To validate these data, we performed quantitative real-time PCR for all nine miRNAs (plus miR-15a as a negative control), using the same exosome-derived RNAs from A-549 and SK-MES and RNA derived from exosomes purified from the supernatant of HEK-293 cells. We confirmed that miR-15a expression was not detectable in the exosomes of any of the three cell lines and that the expression of miR-16 was not significantly different among the three cell lines (Fig. 1*B*). However, the expression of miR-21, -27b, and -29a was significantly higher in exosomes derived from A-549 and SK-MES cells than in exosomes from HEK-293 cells ($P < 0.001$), suggesting a cancer-specific pattern of secreted miRNAs (Fig. 1*B*). The NanoString expression data for miR-133a, –193a-3p, -544, -563, and -1283 were not confirmed by quantitative real-time PCR, and these miRNAs were not considered further.

MiRNAs in Cancer-Released Exosomes Can Reach and Bind TLRs. Because both murine *TLR7* and human TLR8 are located in intracellular endosomes, we first asked whether cell-released exosomes are able to reach TLR-containing endosomes in a "receiving" cell. Therefore, we cocultured HEK-293 cells previously transfected with a plasmid encoding a CD9 exosome marker conjugated with GFP with RAW 264.7 murine macrophages stained with a vital blue cell tracker, in which TLR-containing endosomes also were labeled with red LysoTracker. We observed that RAW macrophages incorporated CD9-GFP exosomes released by HEK-293 cells, and these exosomes colocalized with endosomes in RAW cells (Fig. 2*A*). Next, we asked whether extracellular miR-16, -21, and -29a can reach TLR8 within intracellular endosomes. To this aim, we used Dotap liposomal formulations of the miRNAs of interest (mimicking the exosomes in which they are enclosed). HEK-293 cells, which do not express TLR8, were transfected with a plasmid expressing GFP-tagged TLR8 protein. After 48 h, cells were treated with a

Author contributions: M.F., A.P., F.C., D.P., and C.M.C. designed research; M.F., A.P., F.C., R.G., E.G., R.S., F.L., P.F., G.J.N., N.Z., M.C., D.W., and P.N.-S. performed research; P.N.-S. contributed new reagents/analytic tools; M.F., A.P., F.C., C.M., G.H.O., H.A., and M.A.C. analyzed data; and M.F., A.P., F.C., and C.M.C. wrote the paper.

The authors declare no conflict of interest.

Freely available online through the PNAS open access option.

[1]Present address: Department of Pediatrics and Molecular Microbiology and Immunology, University of Southern California, Keck School of Medicine, Children's Center for Cancer and Blood Diseases, Children's Hospital Los Angeles, Los Angeles, CA, 90027.

[2]M.F., A.P., and F.C. contributed equally to this work.

[3]To whom correspondence may be addressed. E-mail: mfabbri@chla.usc.edu or carlo.croce@osumc.edu.

See Author Summary on page 12278 (volume 109, number 31).

This article contains supporting information online at www.pnas.org/lookup/suppl/doi:10.1073/pnas.1209414109/-/DCSupplemental.

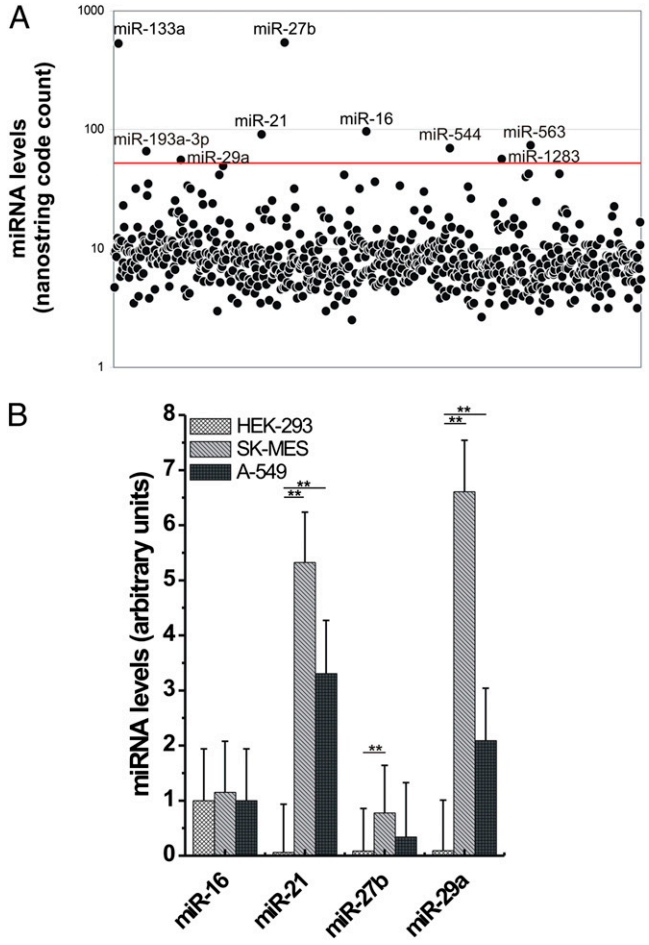

Fig. 1. Levels of miRNAs in exosomes derived from lung cancer cell lines and HEK-293 cells. (*A*) Scatter plot representing the NanoString miRNA profile obtained from A-549 purified exosomes. The red line indicates the threshold of 50 code counts. (*B*) Validation of the NanoString results in A-549 and SK-MES purified exosomes compared with HEK-293 purified vesicles by quantitative real-time PCR. The experiments were conducted in hextuplicate; results are presented as average ± SD. $^{**}P < 0.0001$.

Dotap liposome formulation containing Cy5-conjugated mature miR-16, -21, or -29a, and then blue LysoTracker was added to the culture medium to label cellular endosomes. Colocalization of miRNA, TLR8, and endosomes was detected for all three miRNAs (Fig. 2*B*), suggesting that exogenous miRNAs can reach TLR8 in cellular endosomes. To determine whether these miRNAs bind to TLR8, we performed coimmunoprecipitation assays for TLR8 in HEK-293 cells expressing GFP-TLR8 and treated with Dotap-miR-16, Dotap-miR-21, Dotap-miR-29a, or Dotap alone and determined miRNA levels by quantitative real-time PCR. Although miR-16 was almost undetectable in the GFP-TLR8 coimmunoprecipitate, miR-21 and miR-29a expression was highly enriched (>50-fold) (Fig. 2*C*). We also treated HEK-293 cells expressing GFP-TLR8 with Dotap alone or with Dotap formulations of 5′-biotinylated miR-16, -21, or -29a. As a positive control, we treated cells with 5′-biotinylated ssRNA40, a 20mer ssRNA previously shown to activate TLR8 (12). After coimmunoprecipitation of miRNAs and ssRNA40, we detected TLR8 in the ssRNA40-, miR-21–, and -29a–treated cells (Fig. 2*D*) but not in the cells treated with Dotap alone or with Dotap-miR-16. To investigate whether this interaction also occurs in vivo, we injected B6 mice with Lewis lung carcinoma (LLC) cells, which tend to localize to the lung after injection into the tail, and analyzed lung tumors 15 d after injection. By ISH we showed that miR-29a is produced by cancer cells and not by cells in the adjacent normal lung tissue (Fig. 2*E* and *SI Appendix*, Fig. S1*B*). These findings also were confirmed in samples of human primary lung cancer, where an enrichment of the exosome marker CD9 also was observed in macrophages at the tumor–normal tissue interface (*SI Appendix*, Fig. S2). Also, by locked nucleic acid in situ hybridization (LNA ISH) we observed that miR-29a and exosomes colocalized at the tumor–normal tissue interface in samples of mouse and human lung cancer (Fig. 2*F*), but not in normal tissue, at distance 1 mm from the tumor. Also, we showed that, although miR-29a colocalized with the cancer-associated epithelial marker cytokeratin in the center of the tumor (confirming that cancer cells are the main producers of miR-29a), at the periphery of tumor miR-29a is coexpressed with the macrophage marker F-11, but not cytokeratin, suggesting that miR-29a is present in macrophages at the tumor interface (*SI Appendix*, Fig. S3 *A* and *B*). We also showed that miR-29a colocalized with *TLR7* of the macrophages at the tumor interface (*SI Appendix*, Fig. S3*C*).

Overall, these data indicate that cancer cells secrete miR-29a in exosomes and that this miRNA colocalizes with *TLR7* and TLR8 in macrophages at the tumor–normal tissue interface.

MiRNAs in Cancer-Released Exosomes Functionally Activate TLRs. To determine whether the miRNA–TLR interaction is functional, we assessed whether the miRNAs of interest induce the secretion of cytokines such as TNF-α and IL-6, whose production is increased by TLR activation (12). We isolated peritoneal macrophages from WT and *TLR7*$^{-/-}$ B6 mice (11). Cells were treated with Dotap alone or with Dotap formulations of miR-16, -21, -29a, and -147, and an ELISA for TNF-α and IL-6 was performed. In our functional assays, we included also miR-147 and –574-5p, because they have a mature viral-derived sequence that induces cytokine production through the activation of TLR8 and *TLR7* (12), similar to that of RNA33 (*SI Appendix*, Fig. S4*A*). Although Dotap alone and Dotap–miR-16 did not induce cytokine secretion, miR-21, -29a, and -147 increased TNF-α and IL-6 production in WT but not in *TLR7*$^{-/-}$ mice (Fig. 3 *A* and *B*). We also treated spleen cells from WT and *TLR7*$^{-/-}$ mice with the same miRNAs and assessed expression of CD69, an early activation marker of cells which has a role in inflammation and proliferation (16) and which also is activated by TLR3 (11). Polyinosinic:polycytidylic acid [poly (I:C)], a known agonist of TLR3 (17), served as positive control. Cytofluorimetry showed that miR-21, -29a, and -147, but not miR-16 or Dotap alone, induced CD69 activation in spleen cells from WT but not *TLR7*$^{-/-}$ mice (Fig. 3 *C* and *D*), indicating that these miRNAs induce a *TLR7*-mediated spleen cell activation. To investigate whether miRNA-induced activation of TLRs also occurs in human cells, we performed an NF-κB reporter assay in HEK-293 cells. NF-κB, a transcription factor modulating the expression of several cytokine genes (18), is activated by several TLRs, including the only ssRNA-binding human TLRs, TLR7 and TLR8. Therefore, we treated HEK-293 cells expressing human TLR7 or TLR8 (hereafter, TLR7- and TLR8-HEK-293 cells, respectively) with Dotap alone or with Dotap formulations of miR-16, -21, -29a, or -147 and performed an NF-κB reporter assay. As positive controls we used Gardiquimod and ssRNA40, specific agonists of TLR7 and TLR8, respectively. NF-κB was activated only in TLR8–HEK-293 cells by each of the tested miRNAs except miR-16 (Fig. 3*E*). These results suggest that miRNA-induced NF-κB activation is mediated by TLR8 and not by TLR7 in human cells. To confirm this conclusion, we transfected TLR8-HEK-293 cells with a plasmid encoding a dominant negative form of TLR8 (TLR8DN) and treated these cells with the miRNAs of interest. In TLR8DN cells, the activation of NF-κB by miR-21 and miR-29a was abolished (Fig. 3*F*). Also, we in-

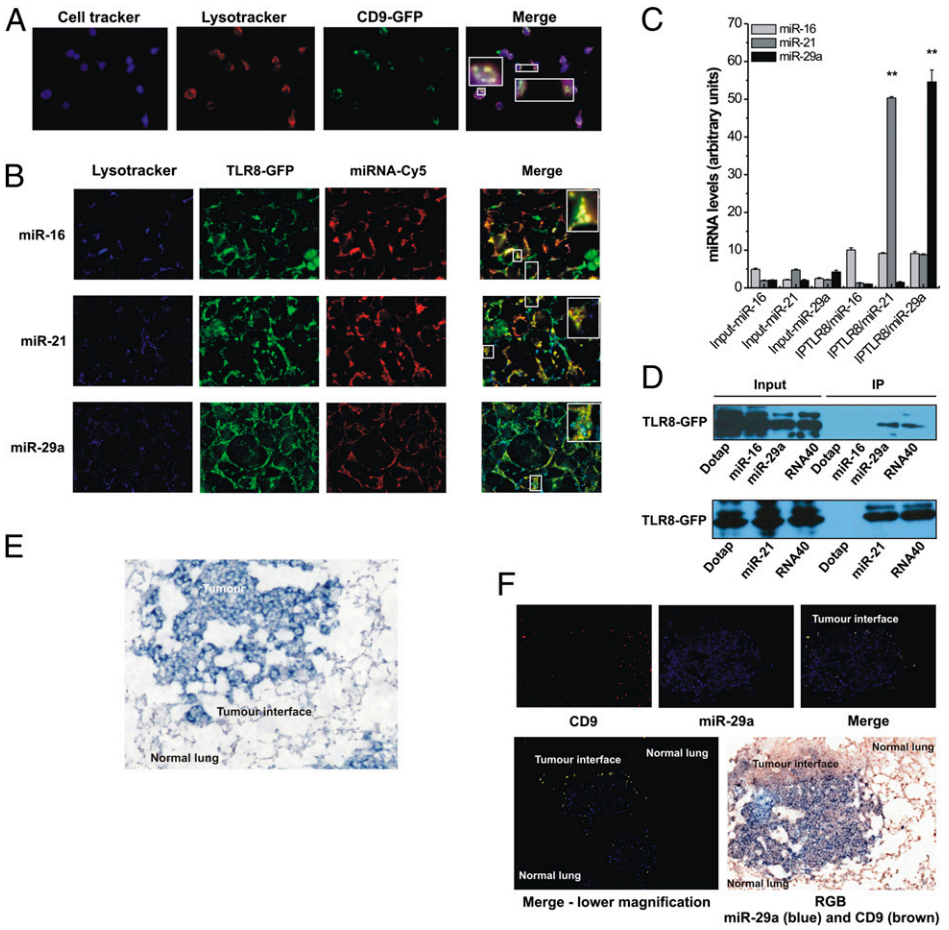

Fig. 2. miR-21 and miR-29a interact with murine *TLR7* and human TLR8 in the endosomes. (*A*) Confocal images of RAW 264.7 cells stained with cell tracker (blue) and with LysoTracker endosome marker (red) and cocultured with HEK-293–secreted CD9-GFP exosomes (green). Colocalization is indicated in yellow (merged image). (*B*) Confocal images of HEK-293 cells cotransfected with endosome LysoTracker (blue), GFP-tagged TLR8 (TLR8-GFP) (green), and Cy5-conjugated mature miRNAs (miRNA-Cy5) (red). Colocalization is indicated in yellow (merged image). (*C*) Levels of miR-16, miR-21, and miR-29a in the coimmunoprecipitates for TLR8 (IPTLR8/miR-16, IPTLR8/miR-21, and IPTLR8/miR-29a, respectively) in TLR8-HEK-293 cells detected by quantitative real-time PCR. Results are shown as means ± SD. $^{**}P < 0.001$. (*D*) Immunoblotting with anti-GFP antibody for TLR8-GFP complex performed on immunoprecipitates derived from TLR8-GFP-HEK-293 cells. (*E*) LNA-ISH for miR-29a (blue) performed on mice tumors. (*F*) (*Upper*) ISH of CD9 (red) and miR-29a (blue) in mouse tumors. Coexpression is indicated in yellow (merged image). (*Lower Left*) Merged image with lower magnification indicates coexpression of CD9 and miR-29a at the tumor interface. (*Lower Right*) Corresponding red/green/blue image (miR-29a is stained in blue and CD9 in brown).

cubated TLR7- and TLR8-expressing human peripheral blood mononuclear cells (PBMCs) from two healthy donors with Dotap alone or Dotap formulations of miR-16, -21, -27b, -29a, -147, –574-5p, or ssRNA40 and performed an ELISA for TNF-α and IL-6. With the exception of PBMCs treated with Dotap alone and with Dotap-miR-16, each of the other miRNAs and ssRNA40 induced the production of TNF-α and IL-6 (Fig. 3 *G*–*J*). Also, in human primary lung tumors we observed coexpression of miR-29a and IL-6 in macrophages at the tumor interface (*SI Appendix*, Fig. S5). Interestingly, at the tumor interface only the miR-29a–positive macrophages were also IL-6 positive (*SI Appendix*, Fig. S5). We also observed that NF-κB pathway activation is required for miR-21– and -29a–induced secretion of TNF-α and IL-6, because phospho-p65 was induced by miR-21 and -29a (but not miR-16), and transfection with IκBα or Iκκ2 dominant negative plasmids reduced TNF-α secretion in RAW 264.7 cells (*SI Appendix*, Fig. S6 *A* and *B*). Overall, the data indicate that miRNAs secreted by lung cancer cells in exosomes can bind to TLR8 in macrophages at the tumor interface and induce TLR8-mediated activation of NF-κB and NF-κB–mediated secretion of proinflammatory cytokines TNF-α and IL-6.

We also asked which structural features in the sequence of miR-21 and -29a confer the capacity to activate TLR8. We observed that, unlike miR-16, both miR-21 and -29a presented a GU motif in the nucleotide region 18–21 (GUUG for miR-21 and GGUU for miR-29a), and GU motifs are predominant in the TLR-activating RNA33 (*SI Appendix*, Fig. S4*A*). Therefore, we disrupted the GU motifs by substituting bases no. 18, 20, and 18+20 in the miR-21 sequence and bases no. 20, 21, and 20+21 in the miR-29a sequence with the corresponding bases of miR-16 for each specific position (*SI Appendix*, Fig. S4*B*). We observed that base no. 20 was very important in modulating TLR-mediated activation of NF-κB for both miR-21 and -29a, whereas the G–U mutation in miR-21 base no. 18 significantly increased miR-21 activation of TLR8 in TLR8-HEK-293 cells (*SI Appendix*, Fig. S6*C*). Overall, the specific nature and position of nucleotides in the mature sequence of miRNAs is involved in TLR activation, although further studies to clarify these aspects are needed.

MiRNAs in Cancer-Released Exosomes Affect Tumor Growth and Spread by Binding and Activating TLRs in Surrounding Immune Cells. LLC cells are not a model of lung metastasis but represent a well-known model of inflammation-related lung cancer

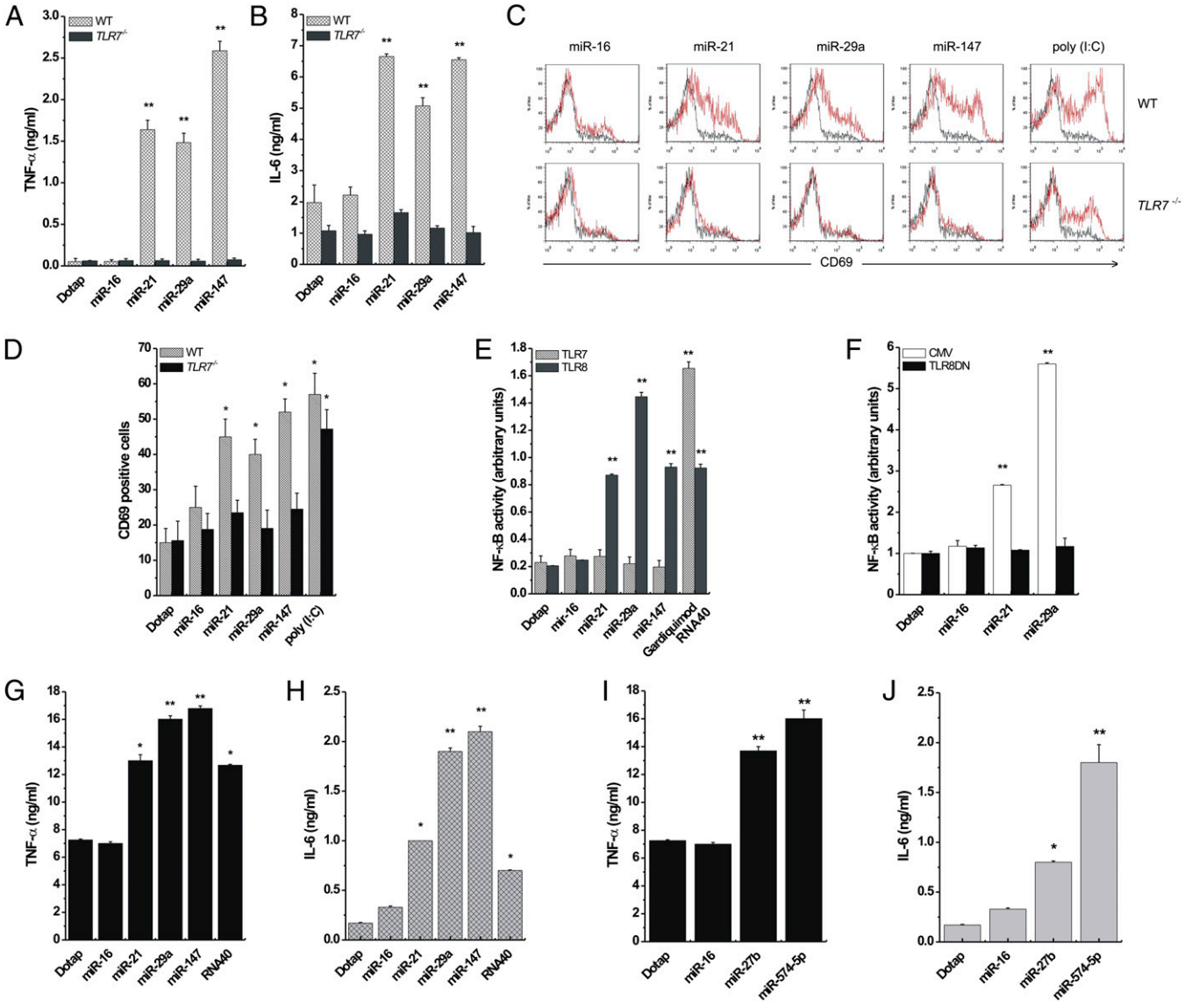

Fig. 3. miR-21, -29a, and -147 induce TLR activation. (*A* and *B*) ELISA for TNF-α (*A*) and IL-6 (*B*) performed on peritoneal macrophages isolated from WT ($n = 4$) and *TLR7*$^{-/-}$ ($n = 4$) mice and treated with Dotap formulations of the indicated miRNAs. (*C*) Flow-cytometric analysis of CD69 in spleen cells of WT and *TLR7*$^{-/-}$ mice treated with the indicated miRNAs. (*D*) Graphic representation of the results presented in *C*. Poly (I:C) was used as a positive control for TLR3-mediated CD69 activation. (*E*) NF-κB activity in TLR7- and TLR8-HEK-293 cells treated with Dotap alone or with Dotap formulations of the indicated miRNAs. Gardiquimod and ssRNA40 were used as positive controls for TLR7- and TLR8-mediated NF-κB activation, respectively. (*F*) NF-κB activity in TLR8-HEK-293 cells transfected with a plasmid encoding a dominant negative form of TLR8 (TLR8DN), or its empty vector counterpart (CMV) and treated with Dotap alone or with Dotap formulations of the indicated mature miRNAs. (*G* and *H*), ELISA for TNF-α (*G*) and IL-6 (*H*) performed on human PBMC isolated from the blood of two healthy donors and treated with Dotap alone or with Dotap formulations of the indicated mature miRNAs. ssRNA40 sequence was used as positive control for TLR8-mediated cytokine secretion. Results in *A*–*H* are shown as means ± SD. $*P < 0.05$; $**P < 0.01$. (*I* and *J*) ELISA for TNF-α and IL-6 performed on human PBMCs treated with Dotap formulations of mature miR-27b and –574–5p for 24 h. Incubation with Dotap alone and with miR-16 was used as negative control. The experiments were conducted in triplicate. Results are presented as average ± SD. $*P < 0.01$; $**P < 0.0001$.

(19). It has been demonstrated that TNF-α secretion induced by the host myeloid cell is important for the formation of multiplicities in the lungs of mice injected with LLC cells (20). Thus, we hypothesized that cytokine secretion induced by immune cells stimulated by lung cancer-secreted miRNAs could be involved in the formation of LLC lung multiplicities. We purified exosomes from the supernatant of LLC and A-549 cells and assessed for miR-16, -21, -27b, and -29a by quantitative real-time PCR. LLC cells released the highest level of miR-16, -21, and -29a (*SI Appendix*, Fig. S7*A*), confirming that these cells represent a good model to test our hypothesis. We cocultured LLC-derived exosomes (or empty medium as a control) with peritoneal macrophages isolated from WT or *TLR7*$^{-/-}$ mice and observed significantly increased TNF-α and IL-6 secretion in the presence of exosomes and in WT versus *TLR7*$^{-/-}$ mice (Fig. 4 *A* and *B*). We also cocultured LLC-derived exosomes (or empty medium as a control) with spleen cells isolated from WT or *TLR7*$^{-/-}$ mice and observed a significantly higher activation of CD69 in the presence of exosomes and in WT versus *TLR7*$^{-/-}$ mice (Fig. 4 *C* and *D*). We finally performed ultracentrifugation of LLC supernatant and cocultured conditioned medium or ultracentrifuged (and presumably exosome-depleted) medium with peritoneal macrophages and spleen cells of WT mice and confirmed that removing exosomes significantly reduced TNF-α and

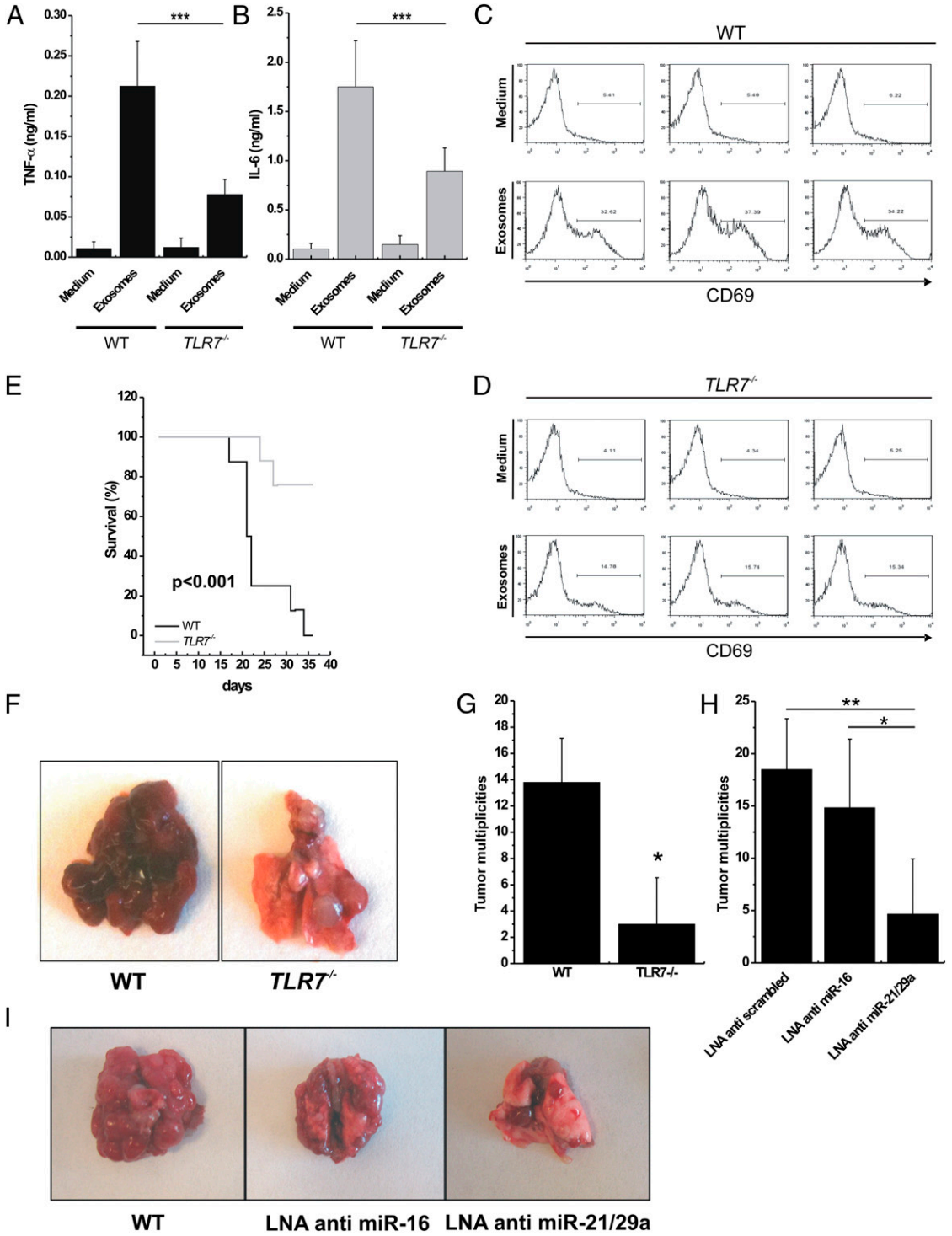

Fig. 4. miRNA-induced *TLR7* activation increases formation of lung multiplicities in mice. (*A* and *B*) ELISA for TNFα (*A*) and IL-6 (*B*) performed on conditioned medium of peritoneal macrophages isolated from WT ($n = 3$) and $TLR7^{-/-}$ ($n = 3$) mice, incubated with RPMI (Medium; negative control) or exosomes purified from LLC cells for 48 h. (*C* and *D*) Flow-cytometric analysis of CD69 in spleen cells isolated from WT and $TLR7^{-/-}$ mice treated as in *A* and *B*. (*E*) Kaplan–Meier curves for WT ($n = 7$) and $TLR7^{-/-}$ ($n = 7$) mice after tail injection of LLC cells. (*F*) Representative images of different tumor multiplicities detected in lungs in the WT and the $TLR7^{-/-}$ mouse groups. (*G*) Tumor multiplicities in the WT and $TLR7^{-/-}$ mouse groups, after tail injection of LLC cells. (*H*) Tumor multiplicities in B6 mice injected with LLC cells transfected with LNA anti-scrambled (control; $n = 6$), LNA anti–miR-16 ($n = 6$), or LNA anti–miR-21/29a ($n = 6$). (*I*) Representative images of lungs in mice injected with LLC cells transfected as indicated. Results in *A*–*E*, *G*, and *H* are shown as means ± SD. $^*P < 0.05$; $^{**}P < 0.01$; $^{***}P \leq 0.005$.

IL-6 secretion by macrophages and CD69 activation by spleen cells of WT mice (*SI Appendix*, Fig. S7 *B*–*D*). Interestingly, some TNF-α and IL-6 secretion and CD69 activation also were observed in $TLR7^{-/-}$ mice in the presence of exosomes, suggesting that these vesicles also carry other signals able to activate cytokine secretion and CD69 activation. We also cocultured LLC-derived exosomes (or ssRNA40 as a positive control) with WT TLR8-HEK-293 cells or with TLR8-HEK-293 cells pretreated

with Bafilomycin A (an antibiotic that perturbates endosomal function) and observed significantly reduced NF-κB activation ($P < 0.0005$) in the presence of Bafilomycin A (*SI Appendix*, Fig. S7*E*). Next, we injected LLC cells into the tails of WT and *TLR7*$^{-/-}$ mice and assessed overall survival of the animals and number of lung multiplicities after necropsy. The Kaplan–Meier curves indicate significantly shorter overall survival of LLC-injected WT mice versus *TLR7*$^{-/-}$ mice ($P < 0.001$) (Fig. 4*E*). Also, lung tumor multiplicities were significantly higher in LLC-injected WT mice than in LLC-injected *TLR7*$^{-/-}$ mice (average number of multiplicities, 13.8 versus 3.8, respectively; $P < 0.05$) (Fig. 4 *F* and *G*). These data confirm the importance of *TLR7* activation in the development of lung cancer multiplicities. Finally, to assess the role of miRNAs released from lung cancer exosomes in *TLR7* activation and in the metastatic process, we silenced the expression of miR-16 or of miR-21 and -29a combined in LLC cells by LNA anti-miRNA inhibitors. After anti-miRNA transfection, the levels of the silenced miRNAs were reduced in the exosomes derived from these cells (*SI Appendix*, Fig. S7*F*). The transfected cells were injected into the tail vein of B6 mice, and lung multiplicities were counted. Mice injected with LLC cells not expressing miR-21/29a in their exosomes formed fewer lung multiplicities (Fig. 4 *H* and *I*). We also observed that WT mice treated with GW4869, an inhibitor of miRNA and exosome secretion (21), produced a significantly lower number of lung multiplicities when injected with LLC cells. This effect could be rescued at least in part when LLC-derived exosomes were injected i.v. in GW4869-treated mice (*SI Appendix*, Fig. S7*G*). We further investigated which miRNAs are expressed in cancer cells and adjacent normal lung tissues in mice injected with anti-scrambled LLCs or anti–miR-21/29a LLCs. As expected, cancer cells in lung tumors developed by mice injected with anti-scrambled LLC were positive for the anti-scrambled oligonucleotide. Interestingly, in mice injected with anti–miR-21/29a LLC cells, all cancer cells localized in the lung were positive for miR-29a expression and negative for the anti–miR-29a oligonucleotide expression (*SI Appendix*, Fig. S8). These findings suggest that only the LLC cells in which miR-29a was not successfully silenced by the LNA anti–miR-21/29a transfection were able to localize to the lung. To exclude the possibility that the observed differences were caused by the effects of miRNA silencing unrelated to their exosome release, we investigated the effects of miR-16 and -21/29a silencing on LLC biology. When miR-16 or miR-21/29a was silenced, no difference was observed in LLC growth curve, cell viability, cell cycle, LLC invasiveness, or LLC migration capabilities or in tumor growth in in vivo xenograft mouse models (*SI Appendix*, Fig. S9).

Our findings show that miR-21 and -29a secreted by tumor cells in exosomes can bind to TLR8 (and *TLR7*) and activate these receptors in immune cells, leading to TLR-mediated NF-κB activation and secretion of prometastatic inflammatory cytokines. It has been shown previously that tumor secretion of the extracellular matrix proteoglycan versican induces a proinflammatory response by activating TLR2:TLR6 complexes in myeloid cells (20). We now show that tumor-secreted miRNAs also participate in the protumoral inflammatory process by activating the TLR8 response on immune cells. As a result, tumor cells tend to generate more lung multiplicities when this paracrine loop is intact. Although LLC are not a model of lung cancer metastasis, and further studies should address the relevance of these findings in mice bearing primary tumors that are prone to form spontaneous metastases, our data identify a mechanism of action of miRNAs as agonists of a specific receptor family and suggest that this mechanism is involved in the tumor microenvironment interaction.

Methods

Cell Culture, Transfection, and Treatment. All cell lines were purchased from American Type Culture Collection unless indicated otherwise. Human HEK-293 cells were maintained using standard conditions and were grown in DMEM (Gibco), supplemented with 10% (vol/vol) FBS. Human HEKBlue-TLR7 and TLR8 293 cells (Invivogen) (indicated as TLR7-HEK-293 or TLR8-HEK-293, respectively) were cultured in DMEM supplemented with 10% (vol/vol) FBS, Normocin (50 μg/mL), Blasticidin (10 μg/mL), and Zeocin (100 μg/mL) (Invivogen).

Human A-549 and SK-MES and murine LLC cells were maintained in RPMI 1640, supplemented with 10% (vol/vol) FBS. RAW 264.7 cells were maintained in DMEM supplemented with 20% (vol/vol) FBS. All cells were transfected using Lipofectamine LTX and Plus Reagent (Invitrogen) following the manufacturer's instructions.

For all experiments, cells were treated with 15 μg of HPLC-purified synthetic miRNAs (Integrated DNA Technologies) complexed with Dotap Liposomal Transfection Reagent (Roche) as previously described (1).

For the experiment with Bafilomycin A, TLR8-HEK-293 cells were seeded in a 24-well plate at a density of 200,000 cells per well. The next day cells were preincubated with 10 nM Bafilomycin A (Sigma) for 30 min and then were treated for 24 h with exosomes purified from LLC cells in the presence or absence of 10 nM Bafilomycin A. Cell supernatants were collected and harvested, and the QUANTI-Blue Assay was performed.

Exosome Purification. Serum-free conditioned medium was collected from all the mentioned cell lines at the indicated time points after cell treatment. Medium then was harvested at 14,000 × *g* for 15 min to eliminate cell debris. Exosomes were precipitated by using exosome precipitation solution (ExoQuick; System Bioscience) following the manufacturer's instructions.

Immunofluorescence. HEK-293 cells were seeded 24 h before transfection onto 60-mm plates and allowed to grow to 50% confluence. Then they were transfected with 1 μg of plasmid encoding GFP-TLR8 (Origene). After 48 h cells were treated with the indicated mature miRNA oligos conjugated to Cy-5 fluorophore as described above, washed four times with PBS, and incubated for 15 min with LysoTracker blue DND-22 (Invitrogen) diluted 1:25,000 in PBS.

For the immunofluorescence experiment with physiological exosomes, HEK-293 cells were transfected with 1 μg of plasmid encoding GFP-CD9 (Origene). After 24 h cells were detached and cocultured with RAW 264.7 cells previously seeded onto a 40-mm coverslip at a density of 700,000 cells/mL and stained with blue cell tracker (Invitrogen). After 30 min of incubation, allowing HEK-293 cells to seed, the coculture was finally stained with LysoTracker red DND-99 (Invitrogen) diluted 1:25,000 in PBS, and coverslips were analyzed with a confocal microscope.

Animals. WT B6 mice, B6 *TLR7*$^{-/-}$ mice, and nude mice were purchased from Jackson Laboratories. Seven WT B6 mice and seven *TLR7*$^{-/-}$ B6 mice matched for age and sex (7 wk-old males) were injected with 1.8×10^6 LLC cells in the tail vein and were followed for survival. Necropsy was performed at the moment of death or when the surviving mice were killed 36 d after injection, and multiplicities of lung metastases were photographed and counted.

The in vivo experiment with LLC cells transfected with anti-miRNAs was conducted in six 7-wk-old male B6 mice per group (total $n = 18$). "LNA anti-scrambled" refers to mice injected with LLC cells transfected with LNA anti-scrambled used as control; "LNA anti–miR-16" refers to mice injected with LLC cells transfected with LNA anti–miR-16; "LNA anti–miR-21/29a" refers to mice injected with LLC cells transfected with LNA anti–miR-21 and LNA anti–miR-29a. Mice were injected with 1.8×10^6 LLC cells in the tail vein and were killed 15 d later. Necropsy was performed, and lung multiplicities were photographed and counted.

The in vivo rescue experiment with LLC cells was conducted in 15 male, 7-wk-old B6 mice. Mice were injected with 1.8×10^6 LLC cells in the tail vein in 300 μL of volume (T_0). After 4 d (T_4) we started i.p. injections of 10 mice with GW4869 (1.25 $mg \cdot kg^{-1} \cdot d^{-1}$), an inhibitor of exosome secretion also able to reduce the content of miRNAs in secreted exosomes, and of five mice with DMSO (a solvent of GW4869) as a control, daily for 5 d consecutively. One week after the first injection of GW4869 (T_{11}), we injected the tails of five of the GW4869-treated mice with 1 mL of exosomes purified from WT LLC supernatant. The same mice received a second injection of LLC-derived exosomes 3 d later (T_{14}). All mice were killed at T_{18}, necropsy was performed, and lung multiplicities were counted.

LLC cells transfected with the above-mentioned anti-miRNAs also were injected s.c. into the left flanks of nine nude mice (8×10^6 cells per mouse,

three mice per condition), and tumor growth was monitored for the following 3 wk. Tumor size was assessed once a week using a digital caliper. Tumor volumes were determined by measuring the length (l) and the width (w) of the tumor and calculating the volume ($V = lw^2/2$).

All procedures used in this study complied with federal guidelines and institutional policies of the Ohio State University Animal Care and Use Committee.

Isolation of Primary Human and Murine Cells. Total splenocytes derived from WT and *TLR7*$^{-/-}$ age- and sex-matched mice were prepared by harvesting the spleen and preparing a single-cell suspension. Red blood cells were eliminated by osmotic lysis using red blood cell lysis buffer (eBioscience). Total splenocytes were seeded in a 96-well plate (1×10^6 cells in 200 μL of medium per well) and then were stimulated with synthetic miRNAs or with purified exosomes for 18 h. Cells were stained with phycoerythrin-conjugated anti-CD69 (BioLegend) antibody and analyzed using FACSCalibur flow cytometer (Becton Dickinson).

Macrophages derived from the peritoneal cavity were isolated from WT and *TLR7*$^{-/-}$ age- and sex-matched mice as previously described (11).

PBMC were isolated from heparinized blood of healthy donors by Ficoll-Paque (Pharmacia) centrifugation ($500 \times g$) following the manufacturer's instructions and were plated immediately for stimulation. Human PBMCs or murine peritoneal macrophages (300,000 cells) were stimulated with synthetic miRNAs for 24 h; then ELISAs for TNF-α and IL-6 were performed on the conditioned media using Multi-Analyte ELISArray Kits (SABiosciences) following the manufacturer's instructions.

Statistical Analysis of Data. Statistical data are presented as mean ± SD unless otherwise specified. Significance was calculated by Student's *t* test or by ANOVA test with Bonferroni correction. Kaplan–Meier survival curves were calculated with the log-rank (Mantel–Cox) method using the SPSS statistics software (IBM).

For the LNA-ISH analysis, mean and SD were calculated by using InStat software, and significance was determined by Student's *t* test via InStat.

ACKNOWLEDGMENTS. We thank Phylogeny, Inc. for performing in situ hybridization in its entirety and locked nucleic acid in situ hybridization experiments and for supporting these experiment; Dr. Cecilia Fernandez-Cymering and Dr. Stefano Volinia for supervision of statistical analysis; and Dr. Kay Huebner for critical reading of the manuscript. This work was supported by National Institutes of Health Grants R21 5R21CA150297 (to P.N.-S.) and R01 CA135030, R01 CA124541, and RC2 CA148302 (to C.M.C.). M.F. is supported by a 2009 Kimmel Foundation Fellowship.

1. Ambros V (2001) microRNAs: Tiny regulators with great potential. *Cell* 107:823–826.
2. Bartel DP (2009) MicroRNAs: Target recognition and regulatory functions. *Cell* 136: 215–233.
3. Croce CM (2009) Causes and consequences of microRNA dysregulation in cancer. *Nat Rev Genet* 10:704–714.
4. Fabbri M, Croce CM (2011) Role of microRNAs in lymphoid biology and disease. *Curr Opin Hematol* 18:266–272.
5. Lawrie CH, et al. (2008) Detection of elevated levels of tumour-associated microRNAs in serum of patients with diffuse large B-cell lymphoma. *Br J Haematol* 141:672–675.
6. Gibbings DJ, Ciaudo C, Erhardt M, Voinnet O (2009) Multivesicular bodies associate with components of miRNA effector complexes and modulate miRNA activity. *Nat Cell Biol* 11:1143–1149.
7. Mitchell PS, et al. (2008) Circulating microRNAs as stable blood-based markers for cancer detection. *Proc Natl Acad Sci USA* 105:10513–10518.
8. Valadi H, et al. (2007) Exosome-mediated transfer of mRNAs and microRNAs is a novel mechanism of genetic exchange between cells. *Nat Cell Biol* 9:654–659.
9. Kogure T, Lin WL, Yan IK, Braconi C, Patel T (2011) Intercellular nanovesicle-mediated microRNA transfer: A mechanism of environmental modulation of hepatocellular cancer cell growth. *Hepatology* 54:1237–1248.
10. Eiring AM, et al. (2010) miR-328 functions as an RNA decoy to modulate hnRNP E2 regulation of mRNA translation in leukemic blasts. *Cell* 140:652–665.
11. Lund JM, et al. (2004) Recognition of single-stranded RNA viruses by Toll-like receptor 7. *Proc Natl Acad Sci USA* 101:5598–5603.
12. Heil F, et al. (2004) Species-specific recognition of single-stranded RNA via toll-like receptor 7 and 8. *Science* 303:1526–1529.
13. Akira S (2001) Toll-like receptors and innate immunity. *Adv Immunol* 78:1–56.
14. Medzhitov R, Janeway C, Jr. (2000) Innate immune recognition: Mechanisms and pathways. *Immunol Rev* 173:89–97.
15. Février B, Raposo G (2004) Exosomes: Endosomal-derived vesicles shipping extracellular messages. *Curr Opin Cell Biol* 16:415–421.
16. Martín P, Sánchez-Madrid F (2011) CD69: An unexpected regulator of TH17 cell-driven inflammatory responses. *Sci Signal* 4:pe14.
17. Alexopoulou L, Holt AC, Medzhitov R, Flavell RA (2001) Recognition of double-stranded RNA and activation of NF-kappaB by Toll-like receptor 3. *Nature* 413: 732–738.
18. Kawai T, Akira S (2008) Toll-like receptor and RIG-I-like receptor signaling. *Ann N Y Acad Sci* 1143:1–20.
19. Lipari M, Lenti L, Di Renzo L, Lombardi D, Pontieri GM (1983) A comparative analysis of macrophage activation in C57B1/6 mice treated with inflammatory compounds or bearing Lewis lung carcinoma. *Ric Clin Lab* 13:413–421.
20. Kim S, et al. (2009) Carcinoma-produced factors activate myeloid cells through TLR2 to stimulate metastasis. *Nature* 457:102–106.
21. Kosaka N, et al. (2010) Secretory mechanisms and intercellular transfer of microRNAs in living cells. *J Biol Chem* 285:17442–17452.